Society for
Mathematical
Biology

ORIGINAL ARTICLE

Effect of population partitioning on the probability of silent circulation of poliovirus

Celeste Vallejo[1] (ORCID) **· Carl A. B. Pearson[2,3] · James S. Koopman[4] · Thomas J. Hladish[5,6]**

1 **Abstract**
2 Polio can circulate unobserved in regions that are challenging to monitor. To assess
3 the probability of silent circulation, simulation models can be used to understand
4 transmission dynamics when detection is unreliable. Model assumptions, however,
5 impact the estimated probability of silent circulation. Here, we examine the impact of
6 having distinct populations, rather than a single well-mixed population, with a discrete-
7 individual model including environmental surveillance. We show that partitioning a
8 well-mixed population into networks of distinct communities may result in a higher
9 probability of silent circulation as a result of the time it takes for the detection of
10 a circulation event. Population structure should be considered when assessing polio
11 control in a region with many loosely interacting communities.

12 **Keywords** Poliovirus · Metapopulation · Markov model · Asymptomatic
13 transmission coherence

✉ Celeste Vallejo
celestervallejo@gmail.com

1   Mathematical Biosciences Institute, The Ohio State University, Columbus, OH 43210, USA

2   Depart of Infectious Disease Epidemiology and Centre for Mathematical Modelling of Infectious
     Disease, London School of Hygiene and Tropical Medicine, Keppel Street, London WC1E 7HT,
     UK

3   South African DSI-NRF Centre of Excellence in Epidemiological Modelling and Analysis
     (SACEMA), Stellenbosch University, Jonkershoek Road, Stellenbosch 7600, South Africa

4   University of Michigan, Ann Arbor, MI 48109, USA

5   Department of Biology, University of Florida, Gainesville, FL 32611, USA

6   Emerging Pathogens Institute, University of Florida, Gainesville, FL 32608, USA

Springer

1 Introduction

Wild poliovirus type 1 (WPV1) remains endemic in two countries (Afghanistan and Pakistan) as hard-to-reach areas within these countries, which include those with an inter-Local Government Area or those with a nomadic population, have low vaccination rates (Bawa et al. 2018; Naeem et al. 2013). In one survey designed to understand the cause of low polio vaccination rates in rural Peshawar, Pakistan, 48.8% of children under 4 years old were found to be completely unvaccinated to polio in 2011 with 13.9% of those surveyed claiming health care workers never visited their village (Naeem et al. 2013). Although some such areas have robust and reliable surveillance systems for monitoring polio-induced acute flaccid paralysis, the primary method by which circulation of polio is detected (Saleem et al. 2016), this may not be the case for all areas with either no or low vaccination coverage.

Determining the continued circulation of polio is further complicated by asymptomatic infections. First infections are typically, and repeat infections almost always, asymptomatic (Koopman et al. 2017). Surveillance methods can increase confidence that polio is no longer circulating, but they are difficult to reliably implement (Mbaeyi et al. 2017; Nnadi et al. 2017; O'Reilly et al. 2012). Simulation models based on our knowledge of polio natural history can be used to reconstruct difficult-to-observe transmission dynamics, and thus assess the probability of prolonged silent circulation in polio-endemic regions (Duintjer Tebbens et al. 2018; Duintjer Tebbens and Thompson 2018; Eichner and Dietz 1996; Kalkowska et al. 2019, 2021, 2018, 2012, 2018; Koopman et al. 2017; Thompson and Kalkowska 2020; Vallejo et al. 2017). Modeling can account for infrequent observed cases and ongoing asymptomatic transmission, providing more accurate estimates for the probability of polio circulation conditional on the timing of the last detected paralytic case. This quantity may be of particular interest to policy-makers. The World Health Organization (WHO) set a threshold of 3 years since a detected paralytic case as one of the criteria for declaring a region polio-free (Henderson 1989). In 1996, Eichner and Dietz were the first to use modeling to assess this threshold in terms of the probability of continued circulation, hereafter the *silent circulation statistic*, under a specific set of model assumptions (Eichner and Dietz 1996). Subsequently, researchers have extended the analysis by relaxing the assumptions in that initial work (Duintjer Tebbens et al. 2019; Kalkowska et al. 2018, 2012, 2018; Vallejo et al. 2019). These relaxations of model assumptions make it possible to more confidently assess this time-based criterion in diverse conditions.

Eichner and Dietz used a Markov chain model with susceptible-infectious-recovered (S-I-R) compartments (Eichner and Dietz 1996). Under their assumptions, the 3-year threshold used for polio elimination declaration was deemed appropriate for the large populations (over 500,000 individuals) that they considered (Eichner and Dietz 1996). The model in (Eichner and Dietz 1996) was modified in Kalkowska et al. (2012) to incorporate seasonality and add a vaccinated class. Under their model's assumptions, the 3-year threshold was also found to be suitable for populations over 500,000. In Vallejo et al. (2019), the authors proposed another Markov chain model which included temporary immunity and the possibility for repeat infection. Under their assumptions, the 3-year threshold was not consistently acceptable for smaller

populations (approximately 20,000 individuals) Vallejo et al. (2019). Although these models varied somewhat, all assumed mass-action transmission and exponentially distributed event waiting times.

One implication of assuming mass-action transmission is that all individuals in the system are equally likely to contact all others. This is a potentially problematic assumption for representing polio in endemic regions such as Pakistan, where people reside in large cities as well as in semi-isolated villages (Demographia World Urban Areas 2020; Baig et al. 2019; Naeem et al. 2013). This partitioned structure needs to be accounted for in order to accurately predict the probability of silent circulation. Of particular interest is the probability of silent circulation beyond the 3-year threshold established by the WHO for polio elimination declaration (Henderson 1989). One way in which the homogeneous population assumption can be relaxed is through the use of a metapopulation (or multi-patch) model. This type of model allows for one large, homogeneously mixed population to be viewed as a collection of sub-populations that can only make contacts within their subgroup, thus modifying the contact pattern. [1]

Models in which the contact pattern is modified by partitioning the population have mainly been used to answer questions related to overall persistence (Andreasen and Christiansen 1989; Etienne and Heesterbeek 2000; Hagenaars et al. 2004). Using a stochastic S-I-R model, Hagenaars et al. found that increasing spatial heterogeneity (or the "patchiness") of the population corresponded to a decrease in disease persistence (Hagenaars et al. 2004). Similarly, Etienne et al. found that increased habitat fragmentation was associated to a decrease in species persistence (Etienne and Heesterbeek 2000). These papers both provide evidence that one large population is more likely to sustain persistence when compared to multiple smaller populations of the same total size.

Duintjer Tebbens et al. put forth one example of a polio-specific metapopulation model (Duintjer Tebbens et al. 2019). Modifying the model in Kalkowska et al. (2012), the authors divided the large population considered in Kalkowska et al. (2012) into two sub-populations. One patch held a population with high vaccination coverage and high paralytic case surveillance. The second patch was one that was under-vaccinated with varying rates of paralytic case detection. Movement between patches varied from isolated (no movement) to well mixed. Among other results, they found that the smaller (500,000 individuals) and isolated subpopulation had a higher probability of silent circulation than the larger (5,000,000 individuals), well-mixed population (Duintjer Tebbens et al. 2019). This metapopulation model was further modified to incorporate more subpopulations with increased regional specificity (Duintjer Tebbens et al. 2018; Duintjer Tebbens and Thompson 2018; Kalkowska et al. 2018) as well as environmental surveillance (ES) (Kalkowska et al. 2019). The primary focus of these papers was to study the effect of heterogeneity in other aspects of polio transmission such as access to vaccination and extent of environmental surveillance, and not on contact patterns.

Here, we use a discrete-individual, multi-patch model to extend past work by considering a non-homogeneous contact structure (Vallejo et al. 2019). We compare a homogeneous contact pattern to a heterogeneous one by partitioning a large population, while preserving the same total population. We also consider the effect that

varying vaccination rates and ES detection probabilities have on the probability of silent circulation within this metapopulation framework.

We show that varying the number of patches changes the estimated probability of silent circulation. After 3 years since a paralytic case, generally the partitioned populations have a higher probability of silent circulation when compared to the non-partitioned population, with an exception in the case of high rates of vaccination. However, the relationship between patch size and silent circulation probability is not monotonic. The results we present suggest that the appropriate case-free period for declaring a region polio-free may need to be adjusted based on both population size and structure. The goal of this work is therefore to illuminate modeling assumptions that may present problems when model results are used to declare regions polio-free. As this model is not detailed enough to directly inform policy, the results presented in this paper should be viewed principally as a guide to addressing the influence of common modeling assumptions.

2 Methods

2.1 Discrete-Individual Stochastic Model Specification

The model used in this paper is an extension of the S-I-R type counting process in Vallejo et al. (2019). The original compartments considered were S: naive suscep- tible, I_1: first infection with the virus, R: recovered and fully immune, P: partially susceptible, and I_r: reinfected. We assume that only individuals in the I_1 compartment experience symptomatic polio, in particular polio-induced acute flaccid paralysis. We extend the model considered in Vallejo et al. (2019) by including a vaccinated com- partment; transmission seasonality; and a population divided into patches, typically p patches each with population size N_p, with and without movement between patches. We assume an "effective" vaccination rate, such that vaccinated individuals in the model cannot be infected. A less-than-perfect vaccine would require higher actual coverage to achieve performance similar to the effective coverage levels we consider. ES is also incorporated as a possible detection system, but has no effect on transmis- sion. To simulate the use of ES in the hypothetical population, we use a detection rate that is the probability of detection via ES multiplied by the number of infected individuals (I_1 and I_r). This is done for each patch and occurs once each day. Although this does not allow us to explore questions related to implementation of ES such as location of ES sites or size of catchment areas, we can use this method to understand how sensitivity of ES affects the probability of silent circulation.

Immunity to polio is parameterized by two terms: waning immunity rate and wan- ing immunity depth. Waning immunity rate refers to the speed at which the immunity wanes (i.e., the average rate at which an individual leaves the recovered class). Wan- ing immunity depth is a unitless quantity that represents the protection offered by antibodies generated from a natural infection. In the model, waning immunity depth is accounted for in the reinfection and recovery rates. Reinfection occurs at a much slower rate on average and recovery occurs at a much faster rate compared to infection and recovery in a naive susceptible individual. For more details, see (Koopman et al.

Table 1 Events and corresponding model transitions. For each compartment, the superscript refers to the patch and the subscript refers to the number in that compartment. All events (with the exception of movement between patches) occur among individuals of the same patch p. Birth and death events are coupled to keep population size constant: a death in any compartment induces a birth in the S compartment in that patch

Event description	Transition
Vaccination	$(S_i, V_j) \rightarrow (S_{i-1}, V_{j+1})$
First infection	$(S_i, I_{1,j}) \rightarrow (S_{i-1}, I_{1,j+1})$
Reinfection	$(P_i, I_{r,j}) \rightarrow (P_{i-1}, I_{r,j+1})$
First infection recovery	$(I_{1,i}, R_j) \rightarrow (I_{1,i-1}, R_{j+1})$
Reinfected recovery	$(I_{r,i}, R_j) \rightarrow (I_{r,i-1}, R_{j+1})$
Immunity waning	$(R_i, P_j) \rightarrow (R_{i-1}, P_{j+1})$
Death in S	No change
Death in $X \in \{I_1, V, R, P, I_r\}$	$(S_i, X_j) \rightarrow (S_{i+1}, X_{j-1})$
Bi-directional movement between patches p, q	$\left(M_i^p, M_j^q\right) \rightarrow \left(M_{i-1}^p, M_{j+1}^q\right)$
$M, T \in \{S, I_1, V, R, P, I_r\}$	$\left(T_k^q, T_l^p\right) \rightarrow \left(T_{k-1}^q, T_{l+1}^p\right)$

146 2017). As in Vallejo et al. (2019), we fix the waning immunity scenario as fast shallow
147 (i.e., immunity wanes quickly but to a shallow depth).

148 Due to the strongly seasonal nature of polio infections (Duintjer Tebbens et al. 2013;
149 Grassly and Fraser 2006; Martinez-Bakker et al. 2015; O'Reilly et al. 2012), we add
150 seasonal forcing to the transmission term of the model given in Vallejo et al. (2019).
151 The form of the seasonal transmission term $\beta(t)$ is given in Eq. 1. The amplitude is
152 chosen to be 5% of the contact rate β to mimic the amount of seasonal forcing used
153 in Kalkowska et al. (2012).

$$\beta(t) = \beta \left(1 + 0.05 \cdot \sin(2\pi t)\right) \tag{1}$$

155 Event descriptions with corresponding transition in the model are given in Table 1
156 and a diagram of the model is given in Fig. 1. For more details on the model in the
157 absence of vaccination, see Vallejo et al. (2019).

158 Movement between patches is a population density-dependent event in the model.
159 Once the patch is chosen, the sizes of the compartments (S, I_1, V, R, P, I_r) are used
160 as weights to determine the kind of individual to move. To ensure that patch size
161 is constant, there is a reciprocal movement from the sink patch to the source patch.
162 Movement from patch p to a randomly chosen patch q is initiated by an individual
163 in patch p with movement rate $\alpha \cdot$ compartment size (i.e., S, I_1, V, R, P, I_r). The
164 corresponding movement from patch q to patch p occurs by randomly choosing an
165 individual from patch q from a compartment chosen with probability proportional
166 to the compartment's size. Individuals are fully characterized by the compartment in
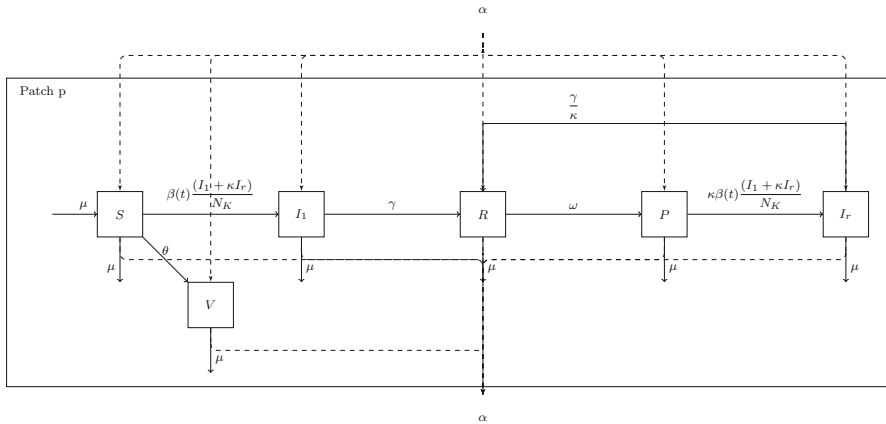167 which they are counted.

Fig. 1 A schematic diagram of the model used in this paper, modified from Vallejo et al. (2019). The compartments of the model are: S (naive susceptible), I_1 (first infection with the virus), V (fully vaccinated against infection), R (recovered and fully immune from infection), P (partially susceptible to infection), and I_r (reinfected). The transmission term ($\beta(t)$) is time dependent to incorporate seasonal forcing. Movement between patches (represented by the dashed lines) is reciprocal to maintain patch sizes

2.2 The Silent Circulation Statistic

The silent circulation statistic is an estimate of the probability of silent circulation given the time interval since the last detected paralytic case of polio. In Vallejo et al. (2019), the authors proposed a formula for estimating the statistic from model output. Slight modifications (in italics) of the definitions used in constructing the formula were necessary in order to apply it to a multi-patch model.

Here, we define an intercase interval to be the time between days when cases were detected anywhere in the population *across all patches*. Note that detected cases may be paralytic or, if ES is occurring, either paralytic or asymptomatic. We define an extinction interval to be the time between the day of the last detected case and extinction (i.e., all infectious compartments empty) *in all patches*. As before, cases may be asymptomatic if ES is occurring. Using this collection of time intervals, we used the following formula (Eq. 2) from Vallejo et al. (2019) to determine the probability of elimination after an interval of Δt years without a detected paralytic case (denoted $P_E(\Delta t)$). Since either polio continues to circulate or polio has been eliminated, the probability of silent circulation given an interval of Δt years without a case ($P_{SC}(\Delta t)$) is $P_{SC}(\Delta t) = 1 - P_E(\Delta t)$.

$$P_E(\Delta t) = \frac{\text{number of extinction intervals} \leq \Delta t}{(\text{number of extinction intervals} + \text{number of intercase intervals} \geq \Delta t)}$$

$$(2)$$

There exist two definitions in the literature for the start of the first intercase interval (Duintjer Tebbens et al. 2019; Eichner and Dietz 1996; Kalkowska et al. 2012, 2018; Vallejo et al. 2019). Either the first intercase interval begins at the start of the simulation

or with the first simulated paralytic case; prior work demonstrated that this assumption does not change the probability of silent circulation estimation in sufficiently large populations (Vallejo et al. 2019), such as those we consider in this work (see Fig. 9 in the Appendix). We assume intercase intervals are only between two explicitly simulated paralytic cases.

2.3 Metapopulation Description

To investigate the consequences of heterogeneous mixing on undetected polio circulation, we compare different partitionings of a population of 64k (64000) individuals: $2 \times 32\,k$ (2 patches of 32000), $4 \times 16\,k$, $8 \times 8\,k$, $16 \times 4\,k$, and $32 \times 2\,k$. The main text figures assume that patches within a model are all equal in size; in Sect. 3.4 and the Appendix we relax this constraint. A population of 64000 individuals is approximately 10% of the population in districts such as Killa Abdullah and Pishin located within the Balochistan Province in Pakistan where polio continues to circulate Naqvi et al. (2017). Considering the potential impact that unvaccinated and under vaccinated subpopulations have in these areas may help to understand why these areas continue to have polio circulation.

2.4 Interpatch Migration Rates

The populations residing within the remaining polio-endemic countries are mobile, migrating both nationally and internationally (Kuschminder and Dora 2009). In 2008, 230,700 people were classified as internally displaced persons within Afghanistan (Kuschminder and Dora 2009). Given a total population of 27.72 million in 2008 in Afghanistan The World Bank (2020), this is an internal movement rate of approximately 0.0083 per year. Notably, there is a long history of migration from Afghanistan to Pakistan Kuschminder and Dora (2009). In 2008, there were approximately 750,000 Afghan refugees living in Pakistan Kuschminder and Dora (2009). Given a total population of 27.72 million in 2008 in Afghanistan The World Bank (2020), the movement rate from Afghanistan to Pakistan is approximately 0.027 per year. While most movement occurs from Afghanistan to Pakistan Kuschminder and Dora (2009), there were a total of 274,200 Afghan refugees that migrated from Pakistan to Afghanistan in 2008 Kuschminder and Dora (2009). Given a total population in Pakistan in 2008 of 171.6 million The World Bank (2020), this gives a movement rate of 0.002 per year from Pakistan to Afghanistan. Movement between tehsils (administrative units) in Pakistan, concentrating on travel to and from Karachi, was captured using cell phone data (Wesolowski et al. yyy). The data captured movement rates ranging from 21.9 per year to 44.04 per year (Wesolowski et al. yyy).

These numbers most likely contain some biases. The national migration rate of Pakistan may be much lower, as the tracked population was described as "highly mobile" (Wesolowski et al. yyy) and necessarily owned a cell phone; cell phone subscribers represented approximately 22% of the total population. It is also possible that the true migration rates between Afghanistan and Pakistan as well as the internal movement rate within Afghanistan are underestimated, as the studies cited above do

not capture non-refugee movement. Given the wide range of estimated movement rates and the focus of the paper on metapopulation dynamics, we chose movement rates to be consistent with observed data while also allowing for multipatch dynamics to remain prominent. The following movement rates were chosen: 0, 0.05, 0.1, 0.2, and 1 per year. See Sect. 3.3 for the effect of movement rate on the metapopulation dynamics.

2.5 Model Iteration Specifics

Previous work assumed that simulations began with a population initialized at the endemic equilibrium, determined analytically for an arbitrarily large population (Duintjer Tebbens et al. 2019; Eichner and Dietz 1996; Kalkowska et al. 2012, 2018; Vallejo et al. 2019). This assumption may not hold for finite populations, however, and real-world polio-endemic regions are not necessarily at endemic equilibrium when observation begins. We address this with a burn-in period before modeling observations. A burn-in period is used in simulation modeling to move the system away from potentially misspecified initial conditions to a state sampled from the system's stationary distribution. Our model is initialized with 99% of the patch population, N_p, in the S compartment and the remaining 1% in the I_1 compartment to replicate the potential start of a polio epidemic. We simulate a 50-year burn-in (without detecting any cases) to reach conditions that represent those at the quasi-steady-state. In order to prevent extinction before the end of the burn-in period (which would correspond to a real-world population that briefly had polio that was never detected), external exposures occur, at a rate of 0.1% of the population per year. All individuals in the total population are equally likely to be exposed during this time. If a susceptible individual (S or P) is drawn, that person becomes infected (i.e., is moved from S to I_1, or from P to I_r). If the individual is not susceptible (I_1, I_r, R, V), then no infection occurs. After the initial 50-year burn-in period, the observation period begins and external exposures no longer occur; conceptually, this might be because surrounding populations external to the model have high vaccination rates and have thus eliminated polio. Figure 10 in the Appendix shows the distribution of starting conditions for each compartment compared to the endemic equilibrium value that comes from the related differential equations model.

The model is simulated using a Gillespie algorithm Gillespie (1977) with 10,000 replicates. As we are looking to represent real-world polio-endemic settings where by definition at least one polio case has been observed, replicates without at least one detected case are repeated as necessary with new random number seeds. Data collection does not begin until after the burn-in period, and ends when all infectious compartments in all patches are zero (i.e., extinction of the virus in the population), or after 100 years, whichever occurs first. Parameter values relating to transmission and vital dynamics are given in Table 2. The paralysis-to-infection ratio (PIR) is commensurate with that for poliovirus serotype 1 (1 case for every 200 I_1 infections). For simplicity, we assume that every paralytic case that occurs is detected; it is worth noting that prior work has demonstrated that lowering the paralytic case detection

Table 2 Parameters used in the model. Parameters related to transmission and vital dynamics taken from Vallejo et al. (2019)

Parameter	Value	Description
β	135	Contact rate (contacts/individual/year)
μ	0.02	Turnover (birth/death) rate $((\text{year})^{-1})$
γ	13	Recovery rate $((\text{year})^{-1})$
ω	0.2	Waning immunity rate $((\text{year})^{-1})$
κ	0.4179	Waning immunity depth
θ	0%; 5%; 20%; 50%	Proportion vaccinated $((\text{year})^{-1})$
ϵ	0%; 0.1%; 1%; 10%	Probability of detection through ES
PIR	0.005	Paralysis to infection ratio (serotype 1)
α	Varies	Movement rate between patches $((\text{year})^{-1})$
p	1; 2; 4; 8; 16; 32	Number of patches
N_k	64k; 32k; 16k; 8k; 4k; 2k	Village size dependent upon number of patches (p)

probability substantially increases the probability of silent circulation Vallejo et al. (2019).

3 Results

3.1 Effect of Partitioning on the Probability of Silent Circulation

We first compare the probability of silent circulation in the large, homogeneously mixed 64k population to isolated (i.e., movement rate $\alpha = 0$) partitions of the large population in the absence of vaccination and environmental surveillance. Figure 2A depicts the probability of silent circulation in each partitioning as calculated by the silent circulation statistic. Figure 2B presents the differential calculated by subtracting the probability of silent circulation at each Δt interval for the partitioned populations from the large 64k population. Positive values correspond to a higher probability of silent circulation in the 64k population; negative values correspond to higher in the comparison scenario. Figure 2C gives the odds ratio of a particular partitioning having a higher probability of silent circulation compared to the 64k population. Values greater than one indicate that it is more likely for the 64k village to have a higher probability of silent circulation at a particular Δt interval compared to the partitioned population.

Initially, up to approximately 2 years since a detected paralytic case of polio, the homogeneously mixed 64k population has a higher probability of silent circulation when compared to the various partitionings. The differential increases monotonically with an increase in the number of partitions. Subsequently, with the exception of 32 patches of 2k, the large population has a lower probability of silent circulation compared to the partitions. This differential, however, does not have monotonic behavior with patch size. The mid-range partitions ($16 \times 4k$ and $8 \times 8k$) emerge as the divisions with the higher probability of silent circulation after 3 years without a detected

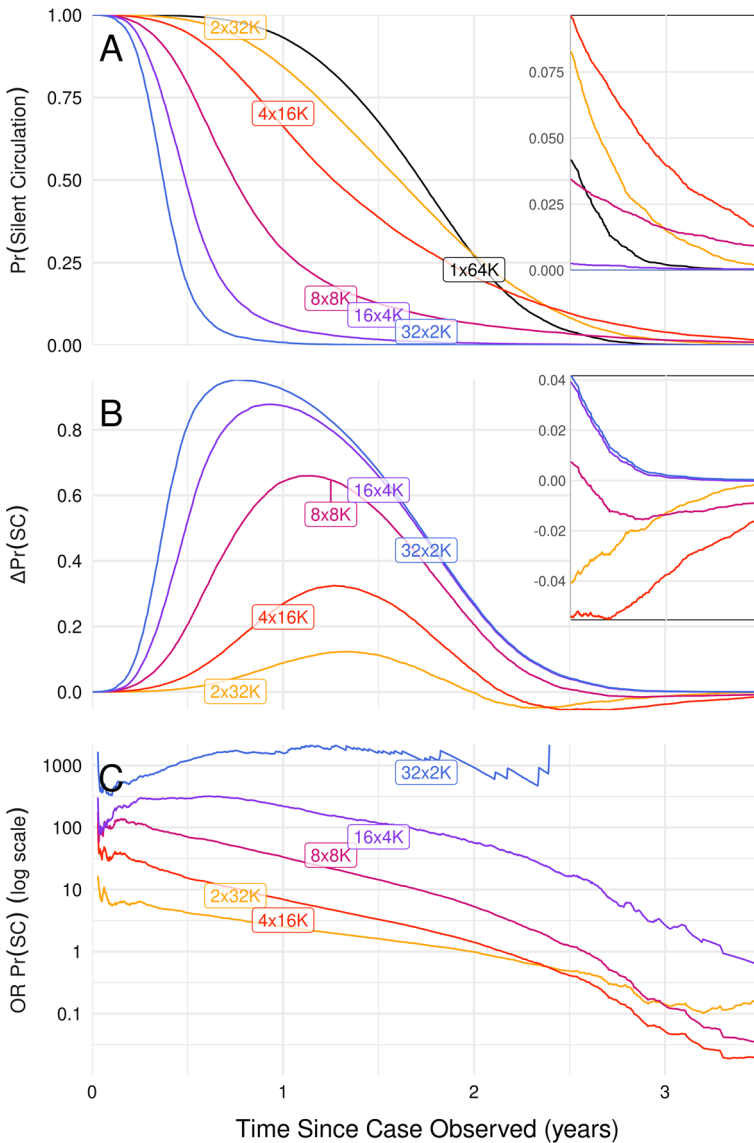🖄 Springer

Fig. 2 Effect of population partitioning on the probability of silent circulation visualized using the silent circulation statistic (**A**), the probability differential (**B**), and the odds ratio (**C**). The probability differential (**B**) is calculated by subtracting the probability of silent circulation in the partitioned populations from that of the large 64k population. Negative values indicate that the partitioned populations have a higher probability of silent circulation. Values less than one in the odds ratio plot (**C**) indicate that the 64k population is less likely to have continued silent circulation compared to the partitioned populations. The inset plots expand the *y*-axis scale to show behavior between 2.5 and 3.5 years since a paralytic case was observed

paralytic case, with $4 \times 16k$ having the highest overall. This indicates that a smaller number of larger isolated patches (such as four isolated villages) have a higher probability of prolonged silent circulation than one homogeneously mixed population (such as a large city).

3.1.1 Intercase and Extinction Interval Distributions

To understand the source of the nonlinear relationship between patch size and silent circulation probability after 3 years since a paralytic case observed in the silent circulation statistic, we consider the intervals used to construct it.

Figure 3A shows the cumulative distribution function (CDF) of intercase interval lengths (time between two detected cases) for all populations considered. The relationship between patch size and intercase interval length is complex. The mid-range populations ($8 \times 8k$ and $4 \times 16k$) identified as having the highest probability of silent circulation after 3 years since a paralytic case also have the greatest density of long intercase and extinction intervals. In general, extinction intervals tend to be longer than intercase intervals, but because there may be many intercase intervals before a single extinction occurs, it is possible that a long interval is most likely to end in another case for a given set of model parameters.

The CDF of extinction interval lengths is given in Fig. 3B. Again, there is a non-monotonic relationship between extinction interval length and number of population divisions. One difference to note in this plot, although the mid-range populations that were found to have the highest probability of silent circulation after 3 years without a paralytic case have a higher density of extinction intervals of length greater than 3 years, 8 patches of 8k overtakes 4 patches of 16k to have the highest overall density during this time. Thus, 8 patches of 8k is more likely to have low levels of persistence before elimination for a longer period of time. Note that the density of extinction intervals for the 64k population is zero at 3 years since a detected paralytic case.

Note that in either case the circulation intervals for the 64k population end before 3 years. This confirms that for large populations the 3-year threshold is appropriate as put forth in (Eichner and Dietz 1996; Kalkowska et al. 2012, 2018; Vallejo et al. 2019). However, this does not seem to be the case for smaller, isolated, and unvaccinated populations as also indicated by Vallejo et al. (2019), as these populations have the potential to have longer times between either a paralytic case or extinction. While intervals greater than 3 years remain uncommon in our simulations, they may become increasingly likely as the number of villages (and total population) increases further, e.g., $\gg 4$ patches of 16k people.

3.2 Comparison to a Single Population

Although similar, the scenario of multiple isolated patches each of size x is not equivalent to more replicates of a single population of size x. In constructing the circulation intervals in the multi-patch scenario, events that end circulation such as a paralytic case or extinction are considered across all patches. In contrast, there is only one patch to consider in the case of a single population. We observe the same pattern in

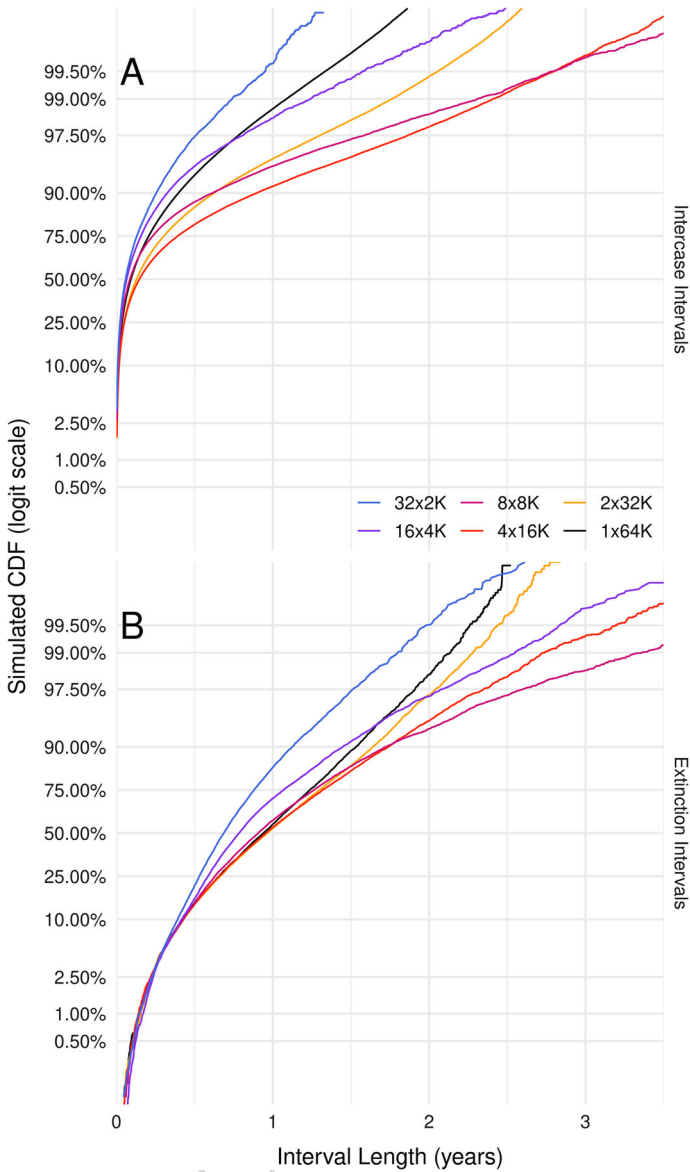$\underline{\textcircled{2}}$ Springer

Fig. 3 Cumulative distribution of intercase (time between detected paralytic cases, **A** and extinction (time between the last paralytic case and extinction, **B** intervals for isolated populations. Intercase intervals beyond 3 years are very rare, while some extinction intervals can last more than 3 years

the intercase and extinction interval distribution by patch size in the single population and isolated multi-patch scenario (see Fig. 11 in the Appendix). However, the isolated multi-patch scenario has longer extinction intervals, while the single population has longer intercase intervals.

3.3 Effect of interpatch movement on the Probability of Silent Circulation

Generally, the subdivided regions described in Sect. 2.3 do not exist in isolation but experience some interpatch movement. In Sect. 3.3.1, we explore the effect of adding interpatch movement on the probability of silent circulation. In Sect. 3.3.2, we compare the silent circulation statistic across all partitions with interpatch movement.

3.3.1 Varying the Movement Rate

Broadly, as the movement rate between patches increases, the probability of silent circulation in the partitioned populations converges to that of the large 64k population (i.e., becomes well-mixed). See Figs. 4 and 5 for two such examples (4×16k and 16×4k, respectively).

For larger populations existing in a smaller number of patches (i.e., 4×16k, Fig. 4), increasing the rate of movement has the effect of decreasing the probability of silent circulation after approximately 2 years since a paralytic case. After 3 years since a paralytic case, 4 isolated patches of 16k have the highest probability of silent circulation when compared to either one large population of 64k or another population of $\times$ 16k that has movement between patches.

On the other hand, in the case of smaller populations existing in a larger number of patches (i.e., 16×4k, Fig. 5) the relationship between movement rate and silent circulation potential is not as straightforward. Similar to the 4×16k population up to 2 years since a paralytic case, increasing movement between patches increases the probability of silent circulation. After 3 years since a paralytic case, the probability of silent circulation is highest for the mid-range of the movement rates considered ($\alpha = 0.05, 0.1,$ and 0.2) and lowest for the extremes of the movement rate range ($\alpha = 0$ and 1).

For both partitionings shown, after 3 years since a case, a large enough movement rate decreased the probability of silent circulation when compared to either some movement or no movement at all. However, the effect of a small amount of movement or complete isolation differed by patch size. For a smaller patch size, a small amount of movement increased the probability of silent circulation when compared to isolated patches, while for a larger patch size, a small amount of movement decreased the probability of silent circulation in comparison with isolated patches. Thus, the structure of the population is important to consider when estimating the silent circulation statistic in a given region, as even adding a small amount of realism (such as movement) can have a significant effect on the predicted outcome.

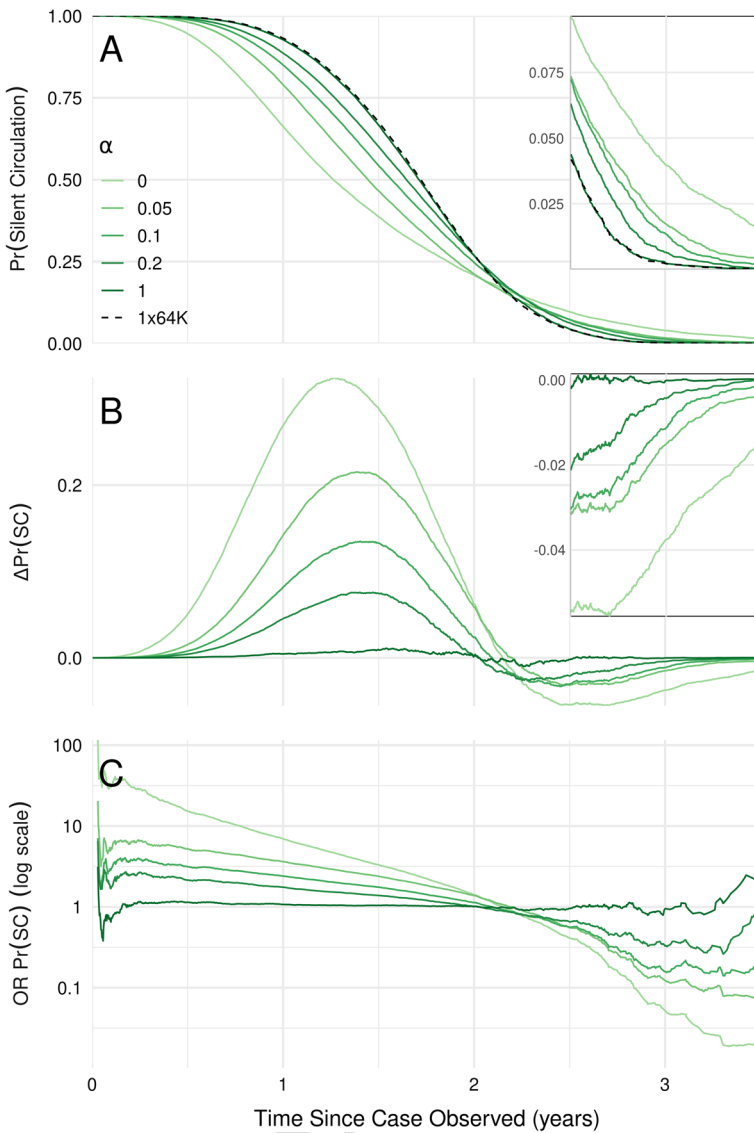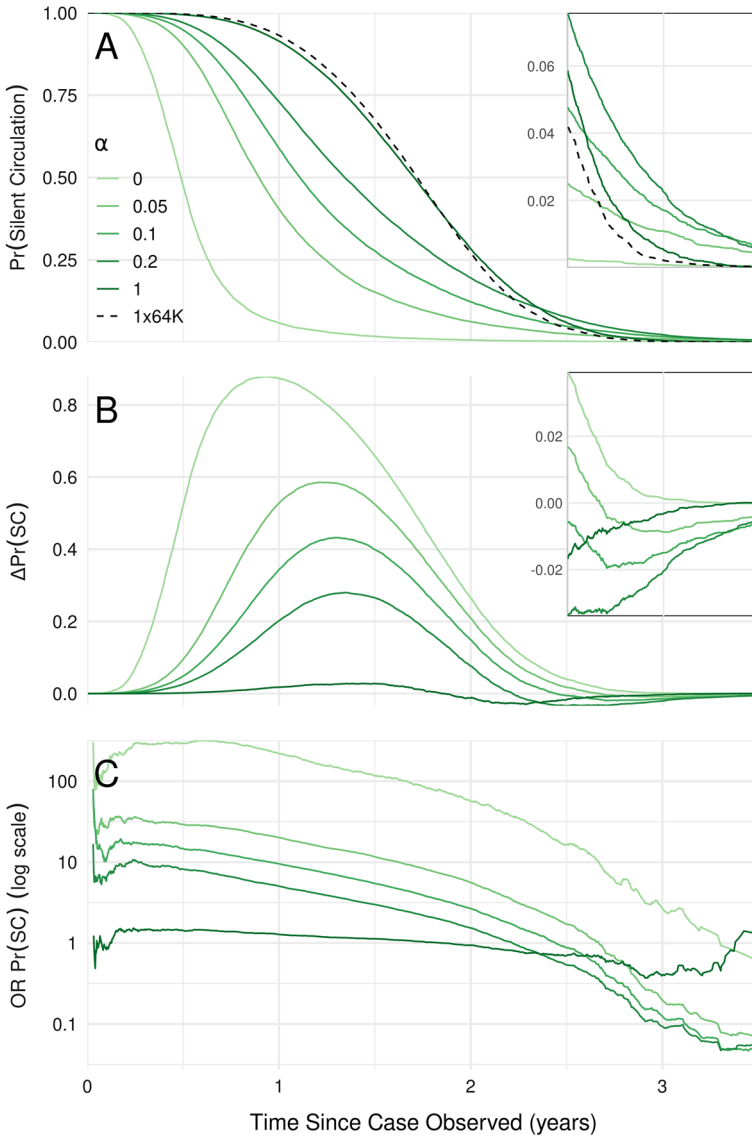**Fig. 4** Effect of interpatch movement on the probability of silent circulation given a Δt interval of time since the last detected paralytic case in the 4 × 16k population visualized using the silent circulation statistic (**A**), the differential comparison to the 1 × 64k population (**B**), and the odds ratio (**C**). The inset plot shows the curves restricted to between 2.5 and 3.5 years since a paralytic case. A movement rate (α) of 0 indicates that the 4 patches are isolated from each other. For the nonzero movement rates, the value indicates the rate at which one individual initiates movement, but with the assumption of reciprocated movement between the sink and the source patch, two individuals move when one initiates

Fig. 5 Effect of interpatch movement on the probability of silent circulation given a Δt interval of time since the last detected paralytic case in the $16 \times 4k$ population visualized using the silent circulation statistic (**A**), the differential comparison to the $1 \times 64k$ population (**B**), and the odds ratio (**C**). The inset plot shows the curves restricted to between 2.5 and 3.5 years since a paralytic case. A movement rate (α) of 0 indicates that the 16 patches are isolated from each other. For the nonzero movement rates, the value indicates the rate at which one individual initiates movement, but with the assumption of reciprocated movement between the sink and the source patch, two individuals move when one initiates

3.3.2 Movement Effect

As can be seen in Figs. 4 and 5 in Sect. 3.3.1 with a large enough interpatch movement rate, the silent circulation curve of the partitioned population converges onto that of the homogeneously mixed population, nullifying the effect of subdividing. To analyze the full influence of partitioning while also considering the impact of interpatch movement, we focus on an interpatch movement rate of 0.1 per year.

Moving from no movement to a movement rate of 0.1 per year had different effects on the probability of silent circulation depending on population size (see Fig. 6; darker lines indicate a movement rate of 0.1 per year and lighter lines are for no-movement scenarios). For smaller patch sizes (e.g., $32 \times 2k$ and $16 \times 4k$), increasing the movement rate increased the probability of silent circulation, while for larger patch sizes (e.g., $2 \times 32k$, $4 \times 16k$, and $8 \times 8k$) increasing the movement rate decreased this probability. With interpatch movement, $8 \times 8k$ had the highest overall probability of silent circulation after 3 years since a detected paralytic case. This shows that there may be a higher probability of undetected circulation in an area with many loosely connected, small villages than there is in an area with one large interconnected village such as a city.

Analogous to the results presented in Fig. 2 (no interpatch movement), the relationship between patch size and circulation potential is not monotonic. This can also be seen in the intercase and extinction interval distribution curves (Fig. 12 in the Appendix).

3.4 Effect of Heterogeneous Patch Sizes on the Probability of Silent Circulation

For the initial analyses on the effect of partitioning a large population on the probability of silent circulation, all subdivided populations were of the same size to simplify extinction dynamics. Redistributing the population such that one patch contained much larger population sizes (e.g., $1 \times 32k$, $4 \times 8k$ or $1 \times 32k$, $8 \times 4k$) uncovered thresholds on the number of smaller-sized patches needed to sustain transmission. For example, one patch of 32k together with 4 patches of 8k with interpatch movement had a lower probability of silent circulation than 8 patches of 8k with interpatch movement (see Fig. 13 in the Appendix). Such thresholds may be important to consider when developing strategies to break transmission chains.

3.5 Effect of Vaccination on the Probability of Silent Circulation

Although our model is conceptually based on isolated sub-populations with minimal effective vaccination coverage, such as may be present in regions with overall high coverage, we also consider the effect of increasing vaccination coverage on silent circulation. Figure 7 shows a comparison of the probability of silent circulation between the $1 \times 64k$ and $4 \times 16k$ populations, with a movement rate of 0.1 per year, for a range of vaccination rates. Overall, the probability of silent circulation decreases as the vaccination rate increases. In this model, vaccinations decrease the number of individuals susceptible to infection, which in turn results in sooner extinction of polio.
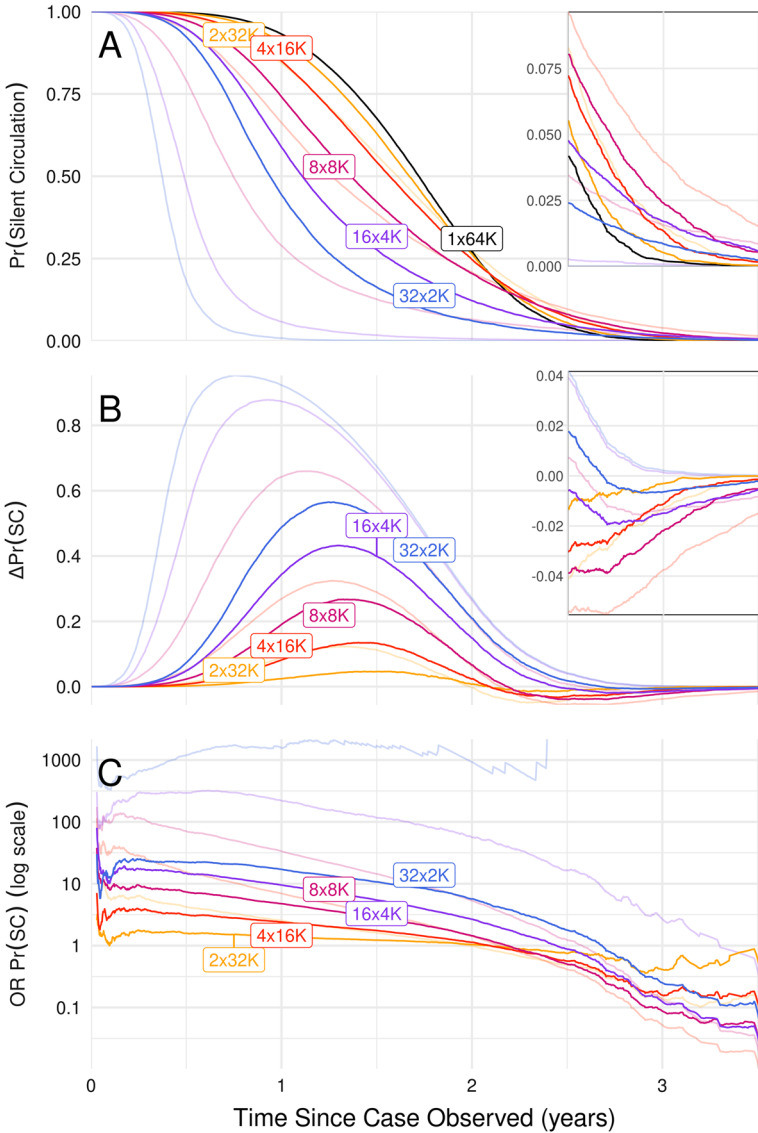
Fig. 6 Comparison of the probability of silent circulation in partitioned populations with a reciprocated movement rate of 0.1 per year visualized using the silent circulation statistic (**A**), the probability differential (**B**), and the odds ratio (**C**). The probability differential (**B**) is calculated by subtracting the probability of silent circulation in the partitioned populations from that of the large 64k population. Negative values indicate that the partitioned populations have a higher probability of silent circulation. Values less than one in the odds ratio plot (**C**) indicate that the 64k population is less likely to have continued silent circulation compared to the partitioned populations. Lighter, more transparent, lines represent the value of the quantity in the absence of movement to use for comparison. The inset plot focuses on behavior between 2.5 and 3.5 years since a paralytic case was observed
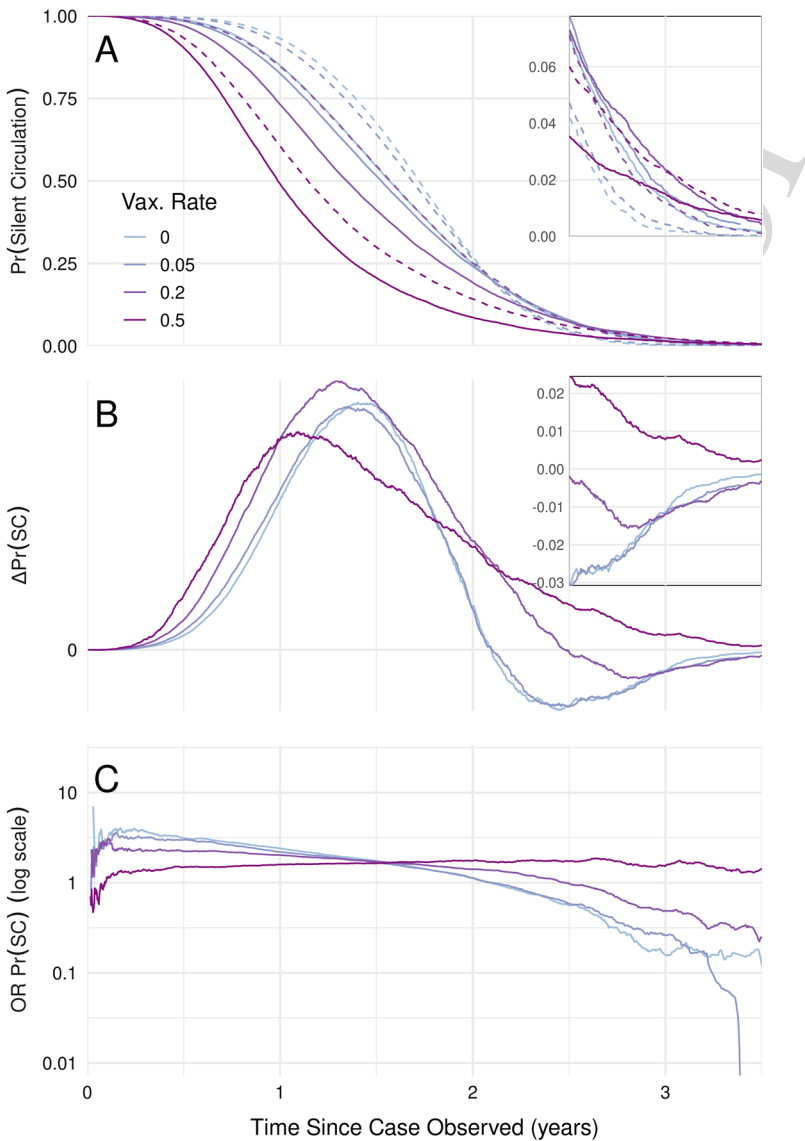
Fig. 7 Comparison of the effect of vaccination on the probability of silent circulation in the 1×64k (dotted lines) and the 4×16k population with movement rate 0.1 per year (solid lines) visualized using the silent circulation statistic (**A**), the probability differential (**B**), and the odds ratio (**C**). The probability differential (**B**) is calculated by subtracting the probability of silent circulation in the partitioned populations from that of the large 64k population. Negative values indicate that the partitioned populations have a higher probability of silent circulation. Values less than one in the odds ratio plot (**C**) indicate that the 64k population is less likely to have continued silent circulation compared to the partitioned populations. The inset plot focuses on behavior between 2.5 and 3.5 years since a paralytic case was observed

At the lower rates of vaccination considered in this model, the 4×16k population with movement still had a higher probability of silent circulation at 3 years since
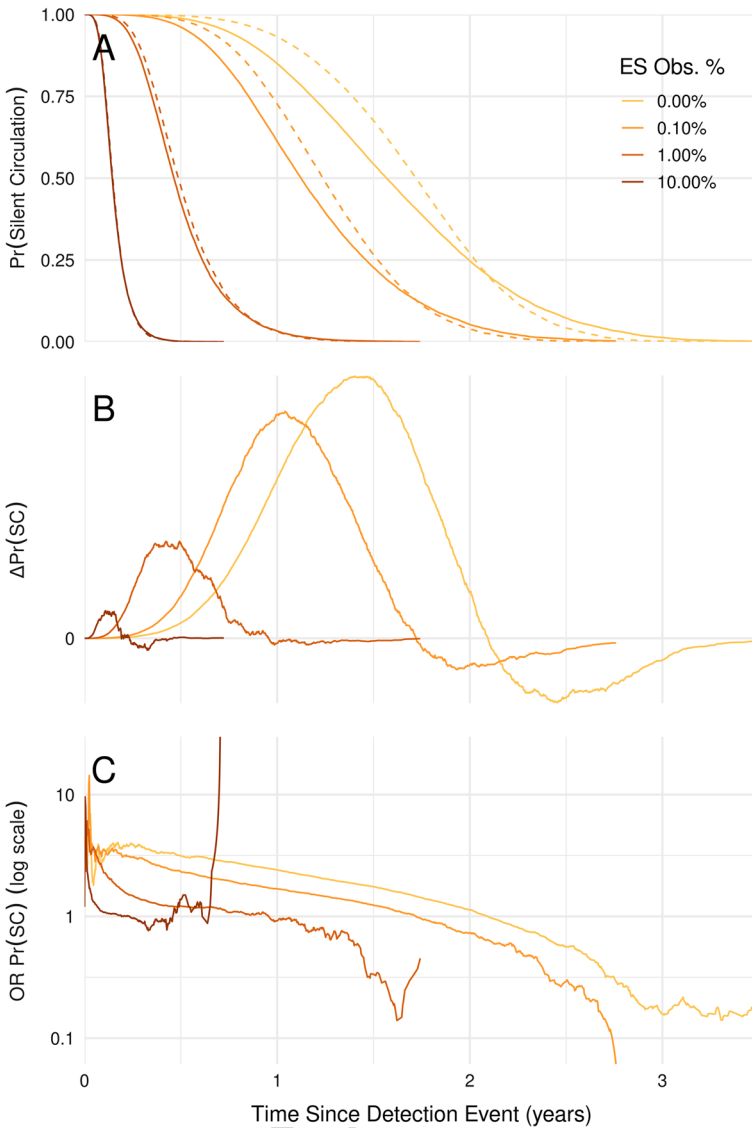
Fig. 8 Comparison of the effect of utilizing environmental surveillance on the probability of silent circulation in the 1x64k (dotted lines) and the 4×16k population with movement rate 0.1 per year (solid lines) visualized using the silent circulation statistic (**A**), the probability differential (**B**), and the odds ratio (**C**). The probability differential (**B**) is calculated by subtracting the probability of silent circulation in the partitioned populations from that of the large 64k population. Negative values indicate that the partitioned populations have a higher probability of silent circulation. Values less than one in the odds ratio plot (**C**) indicate that the 64k population is less likely to have continued silent circulation compared to the partitioned populations. A detection event is defined as detection through either a paralytic case or through ES

a detected paralytic case when compared to the 1×64k population. This was also the case for the isolated and 0.1 per year movement scenarios but in the absence of vaccination. Reducing the susceptible population in accordance with these vaccination

rates was not sufficient to bring the probability of silent circulation in the $4 \times 16k$ population to that of the $1 \times 64k$ population. However, at the highest vaccination rate considered, the $4 \times 16k$ population had the higher probability of silent circulation at 3 years since a detected paralytic case. This provides a threshold for the size of the susceptible population necessary in these four patches in order for the silent circulation potential to be highest in the well-mixed regime versus the segmented population. This further supports the need to consider population structure when utilizing the silent circulation statistic.

3.6 Effect of Environmental Surveillance on the Probability of Silent Circulation

Figure 8 shows a comparison of the probability of silent circulation in the $1 \times 64k$ population with the $4 \times 16k$ population with a movement rate of 0.1 per year for a range of environmental surveillance (ES) detection probabilities. For these scenarios, either a paralytic case or detection via ES are used to construct the intervals of the silent circulation statistic. Instead of considering the probability of silent circulation since a detected paralytic case, we consider the probability since a detection event (circulation detected either through a paralytic case or by ES).

In general, the probability of silent circulation decreases as the probability of detection through ES increases. In particular, the probability of silent circulation was zero at 3 years since a detection event for both population scenarios with at least a 0.1% ES detection probability. Unlike detection of paralytic cases which occurs at a particular rate but only with a first infection, ES can in principle be implemented at any rate and can detect both paralytic and the more common non-paralytic infections.

Increasing the ES detection probability decreased the difference in silent circulation potential between the two population scenarios considered. While this assumes that ES would be as thorough (per capita) in small populations as in large ones—which may not be realistic—this result suggests that having a more thorough ES program reduces the importance of taking population structure into account.

4 Discussion

In this paper, we demonstrate that partitioning a large population can meaningfully change the probability of silent circulation. We found that a large population of 64k had a high probability of elimination after 3 years without a detected paralytic case. While the WHO's elimination criterion does not specify the configuration of the population in its guidelines, these results support using the WHO's elimination criterion of 3 years without a detected paralytic case if the population under consideration is large and well-mixed. However, partitioning this population of 64k, and, in particular, increasing the number of divisions, increased the probability of silent circulation beyond 3 years since a detected case. This suggests that if a population is not well-mixed, the 3-year case-free criterion may warrant more scrutiny.

We show that the frequency of detected cases is the main driver behind longer intervals of time between events that end silent circulation in the partitioned populations.

In particular, prolonged circulation appears to be driven by extinction intervals rather than intercase intervals. In order to decrease these interval lengths, it is important to increase the probability of detecting cases when they occur. As paralytic infections are already likely to be detected, other methods of detection such as environmental surveillance could be used as a supplement Brouwer et al. (2018).

Since this model is not calibrated to an exact region, the time at which changes in silent circulation probability between subpopulations take place should not be the main focus. Nonetheless, the observation that at the 3-year benchmark the relationship between population structure, the amount of interpatch movement, and silent circulation potential can be non-monotonic may be important. Non-monotonicity implies that silent circulation estimation predictions are challenging to make based upon data from other population scenarios. More complex models that take these factors into account and are calibrated to specific populations should be developed in order to better inform policy.

If the silent circulation statistic is to be used to make predictions concerning polio elimination potential in areas with continued circulation, additional work is needed to understand the effect of the assumptions of the data-generating model. For example, the results in this paper confirm the observations in Duintjer Tebbens et al. (2019) when the population is divided into a smaller number of larger patches (e.g., 4 patches of 16k). However, we show that the observation does not hold given a larger number of smaller patches (e.g., 16 patches of 4k).

In this work, we focused on total populations of 64k, with all subpopulations symmetrically connected with one another. For computational reasons, we did not consider substantially larger total populations, but larger, more complex networks of small subpopulations may be able to sustain undetected polio transmission for substantially longer. An important, related operational issue is the scale at which regions are declared polio-free. It is possible that in a sufficiently large, complex population, polio would be sustained, largely undetected, in small refugia, tending to be spread to other such semi-isolated populations before local extinction occurs. These are important considerations for future work.

Additional areas of future investigation include exploration of varying immunity levels, further relaxation of the mass-action transmission term by use of a network model, and considering non-exponential time intervals between events. A clear understanding of how these assumptions affect the probability of silent circulation will produce more accurate estimations. This can be used to understand where transmission may be persistent and highlight the populations in which resource allocation needs to be increased in order to curb the transmission potential.

Data Availability Not applicable.

Code availability The code is available at https://github.com/celestevallejo/polio under the Metapopulation_model folder. The C++ folder contains the simulation model code and the code to calculate the silent circulation statistic using model output. The Model_output folder contains zipped files of all simulation model output used to generate the figures or the silent circulation statistic. The Plotting_scripts folder con-

tains all R scripts used to generate the figures in the manuscript. The SC_statistic_output folder contains zipped files of all output generated from the silent circulation C++ code in the C++ folder.

Declarations

Conflict of interest The authors declare that they have no conflict of interest.

5 Appendix

5.1 Intercase Interval Definition

The initial intercase interval has been defined as either the time between the start of the simulation and the first simulated paralytic case (referred to as the initial case assumption (ICA) in Vallejo et al. (2019)) (Eichner and Dietz 1996; Kalkowska et al. 2012) or as the time between the first two explicitly simulated paralytic cases (referred to as the non-initial case assumption (NICA)) Vallejo et al. (2019). Vallejo et al. (2019) explored the consequence of the ICA in small populations (25000 and smaller). They determined that defining the first interparalytic case interval as the time between the start of the simulation and the first paralytic case had the effect (in most cases) of estimating a higher probability of silent circulation when compared to the NICA. This effect decreased with an increase in population size. In this paper the population size considered is large enough such that either definition of the first interparalytic case interval is appropriate (see Fig. 9). In any case, we believe it is more realistic for observation of the system to begin after a paralytic case had been detected, rather than at the exact moment of detection. Therefore, we define all interparalytic case intervals as between two explicitly simulated paralytic cases (or the NICA).
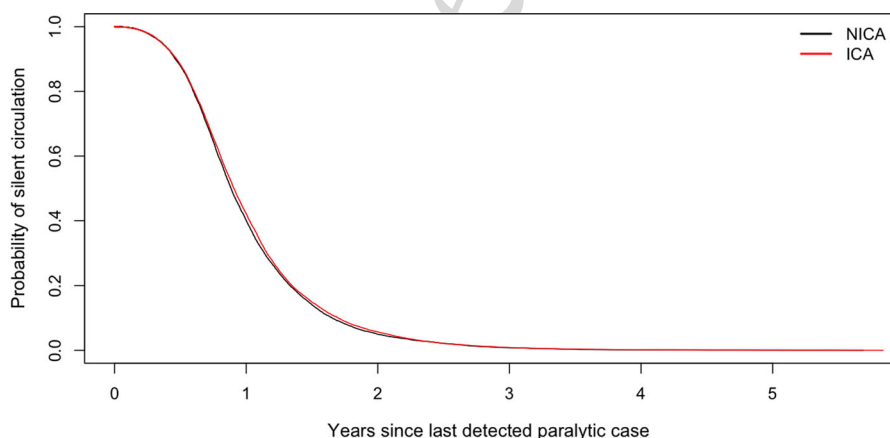

Fig. 9 A comparison of the silent circulation statistic curves with the initial case assumption (defining the time between the start of the simulation and the first simulated paralytic case as an intercase interval; ICA) and without the initial case assumption (defining only the time between explicitly simulated paralytic cases as an intercase interval; NICA) for the 16 patches of 4k scenario. Note that in this paper NICA was used

5.2 Initial Patch Population Distribution
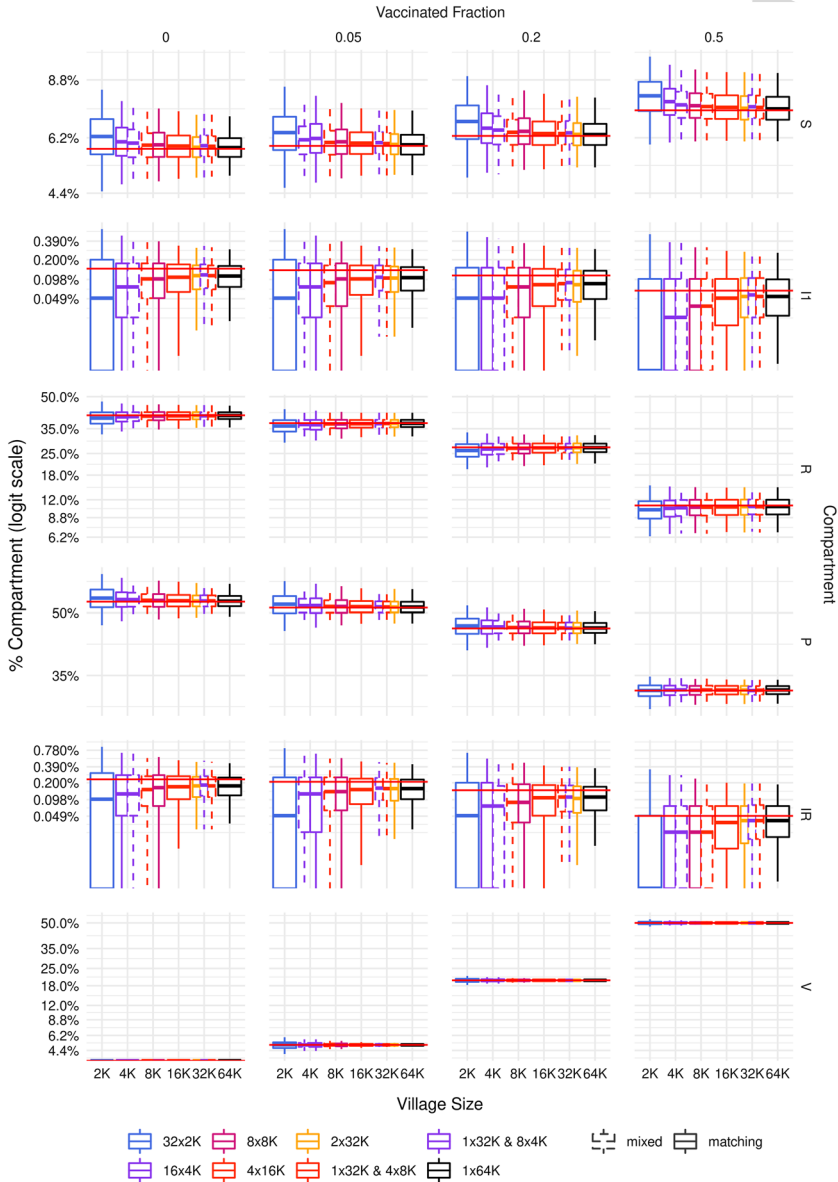
See Fig. 10.

Fig. 10 Box plots demonstrating the distribution of starting values for each compartment after the 50-year burn-in period compared to the endemic equilibrium value obtained by solving the related system of differential equation represented by the solid red horizontal line. Note that the extinction dynamics are highly influential in determining the starting conditions. Even the 64k population is not large enough to reproduce equilibrium-like conditions

5.3 Intercase and Extinction Interval Distribution in Single Populations

See Fig. 11.
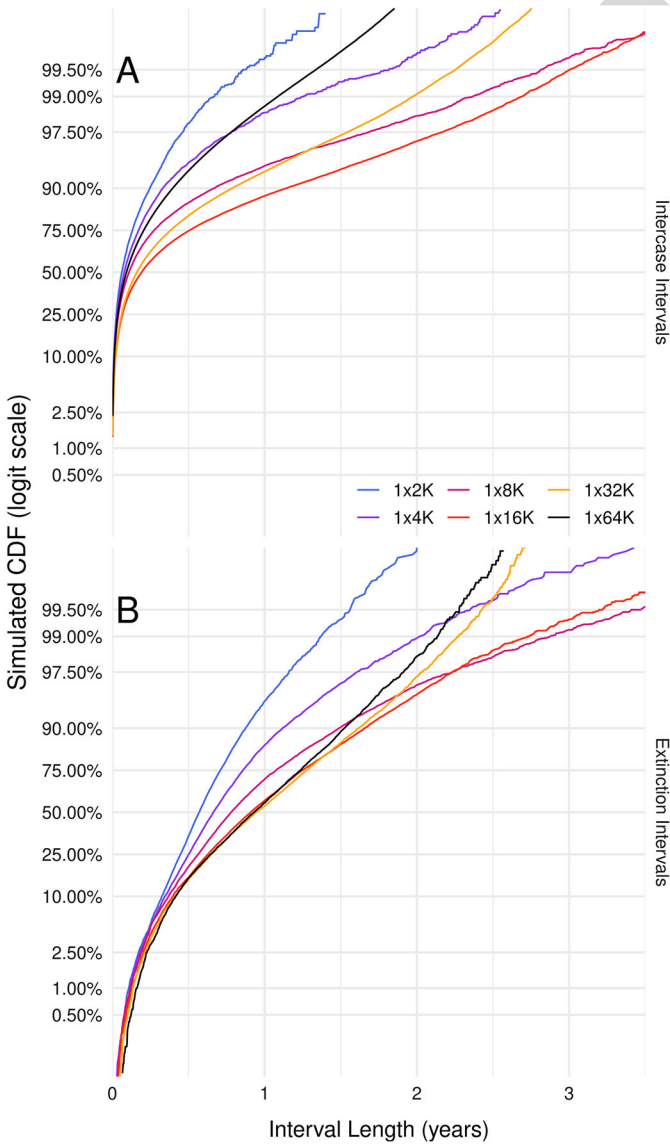
Fig. 11 Cumulative distribution function (CDF) of intercase (time between detected paralytic cases, **A** and extinction (time between the last detected paralytic case and extinction, **B** intervals for single populations

531 ## 5.4 Intercase and Extinction Interval Distribution for the Multi-patch Model with
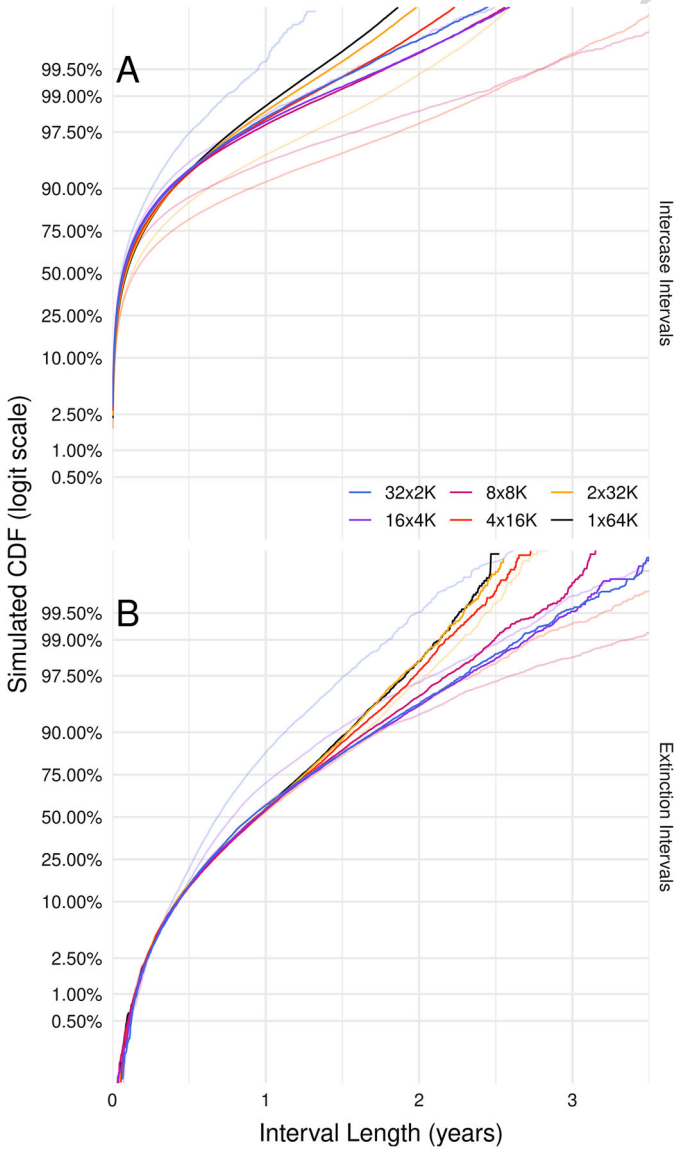532 ## Interpatch Movement

533 See Fig. 12.

Fig. 12 Cumulative distribution function (CDF) of intercase (time between paralytic cases, **A** and extinction (time between the last detected case and extinction, **B** intervals for the multi-patch model with an interpatch movement rate of 0.1 per year. Lighter, more transparent, lines represent the value of the quantity in the absence of movement to use for comparison

5.5 The Probability of Silent Circulation in Heterogeneous Patches

See Fig. 13.
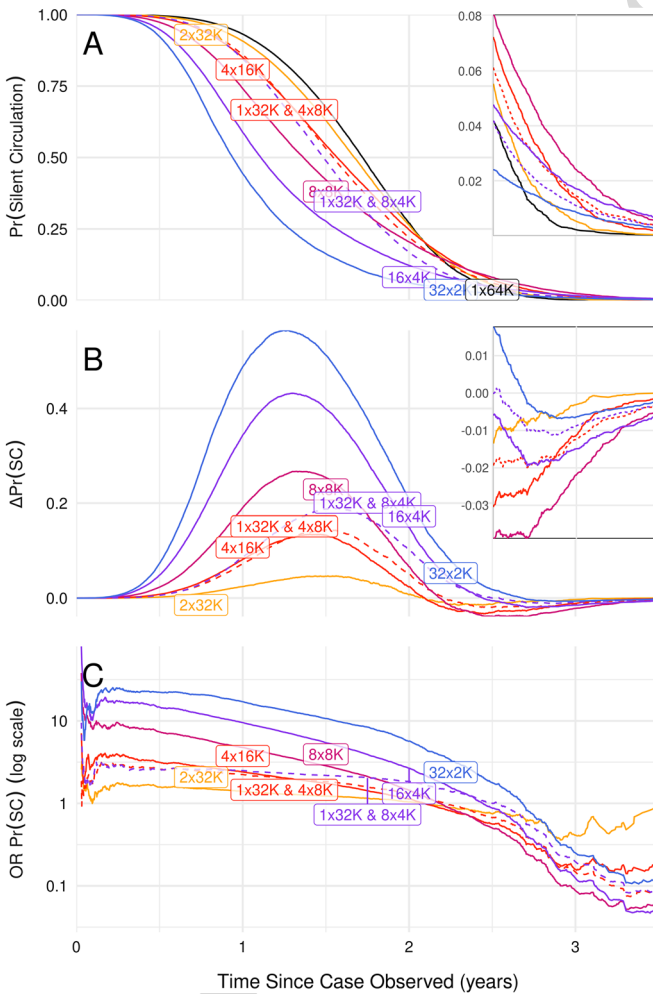
Fig. 13 Comparison of the probability of silent circulation between evenly distributed patch populations and heterogeneous patch distributions visualized using the silent circulation statistic (**A**), the differential comparison to the 1 × 64k population (**B**), and the odds ratio (**C**). The probability differential (**B**) is calculated by subtracting the probability of silent circulation in the partitioned populations from that of the large 64k population. Negative values indicate that the partitioned populations have a higher probability of silent circulation. Values less than one in the odds ratio plot (**C**) indicate that the 64k population is less likely to have continued silent circulation compared to the partitioned populations. The inset plot shows the curves restricted to between 2.5 and 3.5 years since a paralytic case. The mixed population distributions are represented by dashed lines

References

Andreasen V, Christiansen FB (1989) Persistence of an infectious disease in a subdivided population. Math Biosci 96(2):239–253. https://doi.org/10.1016/0025-5564(89)90061-8

Baig IA, Ahmad RN, Baig SA, Ali A (2019) Rural business hub: framework for a new rural development approach in rain-fed areas of Pakistan - A Case of Punjab Province. SAGE Open. https://doi.org/10.1177/2158244019885133

Bawa S, Shuaib F, Saidu M, Ningi A, Abdullahi S, Abba B, Idowu A, Alkasim J, Hammanyero K, Warigon C, Tegegne SG, Banda R, Korir C, Yehualashet YG, Bedada T, Martin C, Nsubuga P, Adamu US, Okposen B, Braka F, Wondimagegnehu A, Vaz RG (2018) Conduct of vaccination in hard-to-reach areas to address potential polio reservoir areas, 2014–2015. BMC Public Health 18(4):1312. https://doi.org/10.1186/s12889-018-6194-y

Brouwer AF, Eisenberg JNS, Pomeroy CD, Shulman LM, Hindiyeh M, Manor Y, Grotto I, Koopman JS, Eisenberg MC (2018) Epidemiology of the silent polio outbreak in Rahat, Israel, based on modeling of environmental surveillance data. PNAS 115(45):E10625–E10633

Demographia World Urban Areas. http://www.demographia.com/db-worldua.pdf. Accessed: 2020-05-16

Duintjer Tebbens RJ, Thompson KM (2018) Evaluation of proactive and reactive strategies for polio eradication activities in Pakistan and Afghanistan. Risk Anal 39(2):389–401. https://doi.org/10.1111/risa.13194

Duintjer Tebbens RJ, Pallansch MA, Kalkowska DA, Wassilak SGF, Cochi SL, Thompson KM (2013) Characterizing poliovirus transmission and evolution: insights from modeling experiences with wild and vaccine-related polioviruses. Risk Anal 33(4):703–749. https://doi.org/10.1111/risa.12044

Duintjer Tebbens R, Pallansch M, Cochi S, Ehrhardt D, Farag N, Hadler S, Hampton L, Martinez M, Wassilak S, Thompson K (2018) Modeling poliovirus transmission in Pakistan and Afghanistan to inform vaccination strategies in undervaccinated subpopulations. Risk Anal 38(8):1701–1717. https://doi.org/10.1111/risa.12962

Duintjer Tebbens R, Kalkowska D, Thompson K (2019) Global certification of wild poliovirus eradication: insights from modelling hard-to-reach subpopulations and confidence about the absence of transmission. BMJ Open 9(1):e023938

Eichner M, Dietz K (1996) Eradication of Poliomyelitis: When Can One Be Sure That Polio Virus Transmission Has Been Terminated? Am J Epidemiol 143(8):816–822

Etienne RS, Heesterbeek J (2000) On optimal size and number of reserves for metapopulation persistence. J Theor Biol 203(1):33–50. https://doi.org/10.1006/jtbi.1999.1060

Gillespie DT (1977) Exact stochastic simulation of coupled chemical reactions. J Phys Chem 81(25):2340–2361

Grassly NC, Fraser C (2006) Seasonal infectious disease epidemiology. Proc R Soc B: Biol Sci 273(1600):2541–2550. https://doi.org/10.1098/rspb.2006.3604

Hagenaars T, Donnelly C, Ferguson N (2004) Spatial heterogeneity and the persistence of infectious diseases. J Theor Biol 229(3):349–359. https://doi.org/10.1016/j.jtbi.2004.04.002

Henderson R (1989) The World Health Organization's plan of action for global eradication of poliomyelitis by the year 2000. Ann N Y Acad Sci 569(1):69–85

Kalkowska DA, Tebbens RJD, Thompson KM (2012) The probability of undetected wild poliovirus circulation after apparent global interruption of transmission. Am J Epidemiol 175(9):936–949

Kalkowska DA, Duintjer Tebbens RJ, Pallansch MA, Thompson KM (2018) Modeling undetected live poliovirus circulation after apparent interruption of transmission: Pakistan and Afghanistan. Risk Anal 39(2):402–413. https://doi.org/10.1111/risa.13214

Kalkowska DA, Tebbens RJD, Thompson KM (2018) Another look at silent circulation of poliovirus in small populations. Infectious Disease Modelling 3:107–117

Kalkowska D, Duintjer Tebbens R, Thompson K (2019) Environmental surveillance system characteristics and impacts on confidence about no undetected serotype 1 wild poliovirus circulation. Risk Anal 39(2):414–425. https://doi.org/10.1111/risa.13193

Kalkowska D, Pallansch M, Wassilak S, Cochi S, Thompson K (2021) Global transmission of live polioviruses: updated dynamic modeling of the polio endgame. Risk Anal 41(2):248–265. https://doi.org/10.1111/risa.13447

Koopman J, Henry CJ, Park JH, Eisenberg MC, Ionides EL, Eisenberg JN (2017) Dynamics affecting the risk of silent circulation when oral polio vaccination is stopped. Epidemics 20:21–36. https://doi.org/10.1016/j.epidem.2017.02.013

Kuschminder K, Dora M (2009) Migration in Afghanistan: History, Current Trends and Future prospects. Ph.D. thesis

Martinez-Bakker M, King AA, Rohani P (2015) Unraveling the transmission ecology of polio. PLoS Biol 13(6):1–21. https://doi.org/10.1371/journal.pbio.1002172

Mbaeyi C, Ryan MJ, Smith P, Mahamud A, Farag N, Haithami S, Sharaf M, Jorba JC, Ehrhardt D (2017) Response to a large polio outbreak in a setting of conflict - middle east, 2013–2017. Morbidity and mortality weekly report, Centers for Disease Control and Prevention

Naeem M, Adil M, Abbas S, Khan M, Naz M, Khan A, Khan M (2013) Coverage and causes of missed oral polio vaccine in urban and rural areas of Peshawar. J Ayub Med College, Abbottabad?: JAMC 23:98–102

Naqvi A, Naqvi S, Yazdani N, Ahmad R, Ahmad N, Zehra F (2017) Understanding the dynamics of poliomyelitis spread in Pakistan. Iran J Public Health 46(7):997–998

Nnadi C, Damisa E, Esapa L, Braka F, Waziri N, Siddique A, Jorba J, wa Nganda G, Ohuabunwo C, Bolu O, Wiesen E, Adamu U (2017) Continued endemic wild poliovirus transmission in security-compromised areas – Nigeria, 2016. Morbidity and mortality weekly report, Centers for Disease Control and Prevention

O'Reilly KM, Durry E, ul Islam O, Quddus A, Abid N, Mir TP, Tangermann RH, Aylward RB, Grassly NC (2012) The effect of mass immunisation campaigns and new oral poliovirus vaccines on the incidence of poliomyelitis in Pakistan and Afghanistan, 2001–11: a retrospective analysis. The Lancet 380(9840):491–498. https://doi.org/10.1016/S0140-6736(12)60648-5

Saleem M, Haider I, Ajmal F, Khan A (2016) Audit & Evaluation of the Acute Flaccid Paralysis Surveillance System in Khyber Pakhtunkhwa, Pakistan. KHYBER MEDICAL UNIVERSITY JOURNAL **8**(1)

The world bank: population, total - Afghanistan, Pakistan (2020). Data retrieved from https://data.worldbank.org/indicator/SP.POP.TOTL?end=2008&locations=AF-PK&start=2008

Thompson K, Kalkowska D (2020) Review of poliovirus modeling performed from 2000 to 2019 to support global polio eradication. Expert Rev Vaccines 19(7):661–686. https://doi.org/10.1080/14760584.2020.1791093

Vallejo C, Keesling J, Koopman J, Singer B (2017) Silent circulation of poliovirus in small populations. Infect Dis Modell 2:431–440

Vallejo C, Pearson CAB, Koopman J, Hladish TJ (2019) Evaluating the probability of silent circulation of polio in small populations using the silent circulation statistic. Infect Dis Modell

Wesolowski A, Qureshi T, Boni MF, Sundsøy PR, Johansson MA, Rasheed SB, Engø-Monsen K, Buckee CO (2015) Impact of human mobility on the emergence of dengue epidemics in Pakistan. Proc Natl Acad Sci 38:11887–11892. https://doi.org/10.1073/pnas.1504964112